Load Change Characteristics of the Discharge Structure in Noble Gas MHD Channels

Takehisa Hara* and Juro Umoto†
Kyoto University, Kyoto, Japan

The two-dimensional, time-dependent behavior of the inhomogeneous plasma in nonequilibrium MHD generators has been numerically calculated. The development of streamers as typical discharge structures is simulated. A cesium-seeded argon plasma is considered. The numerical conditions used in the calculations are set equal to the experimental conditions used in the Eindhoven shock tube facility. It is found that under conditions of relatively large load resistance, an ionization instability occurs in the channel and the final discharge becomes inhomogeneous, wherein a streamer structure is formed. When the load resistance is decreased to a certain value, an almost homogeneous and stable discharge is eventually achieved throughout the channel, even though at the first moment the ionization instability has occurred and streamers have been formed in the channel. Once they are formed, the streamers grow wider and cover the entire region of the channel. The effective electrical conductivity in this case approaches the ideal value of the electrical conductivity calculated from the assumption of no instability. This indicates the possibility of obtaining a plasma with a homogeneous and stable discharge in the channel by selecting the appropriate load condition. By further decreasing the load resistance, both cesium and argon ionize in some parts of the channel and the discharge structure in the channel becomes inhomogeneous.

Nomenclature

B = magnetic induction
E = electric field
E^* = induced electric field
e = charge of the electron
h = channel height
I_L = load current
j = current density
K = load factor of generator
k = Boltzmann's constant
$\boldsymbol{k}$ = wave vector
k_{fa} = ionization rate coefficient of argon atoms
k_{fc} = ionization rate coefficient of cesium atoms
k_{ra} = recombination rate coefficient of argon atoms
k_{rc} = recombination rate coefficient of cesium atoms
M = flow Mach number
m_e = mass of an electron
m_j = mass of species j
n_a = argon atom number density
n_{ia} = argon ion number density
n_c = cesium atom number density
n_{ic} = cesium ion number density
n_e = electron number density
n_{e0} = electron number density at Saha equilibrium
n_{e1} = first-order perturbation in the electron number density
P_d = electrical output density of a generator
p_e = electron pressure
p_s = stagnation pressure
Q_j = momentum transfer cross section of electrons with species j
Q_R = radiation loss
q_e = electron heat flux
r = spherical coordinate
R_L = load resistance
s = electrode pitch
T = heavy species temperature
T_e = electron temperature
T_{e0} = electron temperature at Saha equilibrium
T_s = stagnation temperature
t = time
$\boldsymbol{u}$ = heavy species flow velocity
$\boldsymbol{u}_e$ = electron drift velocity
V_L = load voltage
w = channel width
β = Hall parameter
β_{eff} = effective Hall parameter
β_{cr} = critical Hall parameter
ϵ = seed fraction
ϵ_{ia} = ionization potential of argon
ϵ_{ic} = ionization potential of cesium
ν_j = collision frequency of electrons and species j
σ = electrical conductivity
σ_{eff} = effective electrical conductivity
ψ = current stream function

Introduction

IN nonequilibrium MHD plasmas, perturbations in the electric field and current due to inhomogeneities in the plasma properties result in a nonuniform Joule dissipation that can, in turn, locally affect the plasma properties and lead in some circumstances to unstable situations. This is well known as the ionization instability of MHD plasmas, experimental evidence of which has been found in various studies.[1,2] In recent years, inhomogeneous discharge structures have been observed and the behavior of the unstable plasmas has been made clear by experiments in the Eindhoven shock tube MHD generator.[3,4]

In order to predict the performance of nonequilibrium MHD generators, both experimental studies of the ionization instabilities and theoretical investigations are of importance. The theoretical investigations have been performed both analytically[5-7] and numerically[8-10] by many researchers. Among the theoretical investigations, the analytical ones can predict whether the instability develops in a plasma, but cannot predict the behavior of the plasma after the instability develops. On the other hand, time-dependent numerical simulation studies make it possible to follow the behavior of

Received Dec. 17, 1981; revision received July 20, 1983.

*Associate Professor, Department of Electrical Engineering.
†Professor, Department of Electrical Engineering.

the plasma after it becomes unstable. One of the aims of this study is to investigate numerically how the inhomogeneous discharge structure grows and its final state in the channel. The electron density and the electron temperature distributions inside and outside of the streamers are also of interest.

The idea of obtaining stable plasmas by keeping them in the regime of a fully ionized seed was proposed[11] and experiments to produce the plasmas in this regime by controlling the load conditions have been performed.[12,13] However, the plasmas are not fully ionized at the initial instant for any of the load conditions since the stagnation temperature of the practical situation is around 2000 K. Consequently, it seems from analytical studies that ionization instability occurs and leads to inhomogeneous discharges in the channel. Time-dependent simulation studies make it possible to find the final structure of the plasma to which the instability grows. The second aim of this study is to investigate the possibility of obtaining a stable plasma throughout the channel by selecting the appropriate load condition.

A two-dimensional, time-dependent mathematical model and its numerical procedure in which only cesium was considered to ionize was developed. The growth of streamers in the channel as typical discharge structures was simulated by our previous work.[14] In the present study, both cesium and argon are considered to ionize in order to investigate the discharges under the fully ionized seed conditions.[15]

Theoretical and Numerical Model

Basic Equations

The working medium in a closed-cycle MHD generator consists of a noble gas with a small amount of seed material added. In the present work, the plasma consists of argon seeded with cesium. The plasma temperature ranges 1000-2000 K and has a pressure of several atmospheres. Between these limits the plasma consists of electrons, singly ionized argon and cesium ions, and argon and cesium atoms. In the usual MHD approximations, i.e., low magnetic Reynolds number and charge neutrality, the governing equations of the plasma are the following:

$$j+\frac{\beta}{B}(j\times B)=\sigma\left(E+u\times B+\frac{\nabla pe}{n_e}\right) \tag{1}$$

$$\nabla\cdot j=0 \tag{2}$$

$$\nabla\times E=0 \tag{3}$$

$$n_e=n_{ia}+n_{ic} \tag{4}$$

$$\frac{\partial}{\partial t}n_{ia}+\nabla\cdot(n_{ia}u)=k_{fa}n_en_a-k_{ra}n_e^2n_{ia}=\dot{n}_{ia} \tag{5}$$

$$\frac{\partial}{\partial t}n_{ic}+\nabla\cdot(n_{ic}u)=k_{fc}n_en_c-k_{rc}n_e^2n_{ic}=\dot{n}_{ic} \tag{6}$$

$$\begin{aligned}&\frac{\partial}{\partial t}\left[n_{ia}\left(\frac{3}{2}kT_e+\epsilon_{ia}\right)+n_{ic}\left(\frac{3}{2}kT_e+\epsilon_{ic}\right)\right]\\&+\nabla\left\{\left[n_{ia}\left(\frac{3}{2}kT_e+\epsilon_{ia}\right)+n_{ic}\left(\frac{3}{2}kT_e+\epsilon_{ic}\right)\right]u_e\right\}\\&=j\cdot E-\nabla\cdot(p_eu_e)-\frac{3}{2}\delta n_em_ek(T_e-T)\\&\times\left(\frac{\nu_a}{m_a}+\frac{\nu_{ia}}{m_{ia}}+\frac{\nu_c}{m_c}+\frac{\nu_{ic}}{m_{ic}}\right)\end{aligned} \tag{7}$$

where

$$\sigma=e^2n_e/m_e\nu_e \tag{8}$$

$$\beta=eB/m_e\nu_e \tag{9}$$

$$p_e=n_ekT_e \tag{10}$$

$$j=n_ee(u-u_e) \tag{11}$$

$$k_{ra}=1.29\times10^{-44}\left(11.5\frac{e}{kT_e}+2\right)\exp\left(4.25\frac{e}{kT_e}\right) \tag{12}$$

$$k_{fa}=2.90\times10^{22}T_e^{3/2}\exp(-\epsilon_{ia}/kT_e)\cdot k_{ra} \tag{13}$$

$$k_{rc}=2.58\times10^{-39}\exp[1.337(e/kT_e)] \tag{14}$$

$$k_{fc}=2.42\times10^{21}T_e^{3/2}\exp(-\epsilon_{ic}/kT_e)\cdot k_{rc} \tag{15}$$

$$\nu_j=n_jQ_j(8kT_e/\pi m)^{1/2} \tag{16}$$

$$\nu_e=\sum_{j=1}^{4}\nu_j \tag{17}$$

where $j=1$, 2, 3, or 4 denotes argon atoms, argon ions, cesium atoms, or cesium ions, respectively. The electron-atom cross sections for argon and cesium are taken to be 0.280×10^{-20} $(1.46\times10^{-3}T_e-0.535)$ m^2 and 0.5×10^{-17} m^2, respectively. The electron-ion collision cross section is taken from Spitzer.[16] In these equations the following assumptions are made: 1) the velocities and temperatures are equal for the ions and neutrals, 2) only single ionization of argon and cesium by electron-atom collisions and three-body recombinations are considered, and 3) collisions between the electrons and atoms (by which energy is transferred) are assumed to be elastic.

Two-Dimensional Model

The physical processes of the growth of streamers can be studied in a two-dimensional approximation. The calculations are made in the plane perpendicular to the direction of the magnetic field. The coordinate system and channel geometry used in the calculations are shown in Fig. 1. Here, the following additional assumptions are made:

1) The heavy particle temperature T is constant in space and time.

2) The heavy particle velocity has the form $u=(u,0,0)$ and u is constant in space and time.

3) The magnetic field has the form $B=(0,0,B)$ and B is constant in space and time.

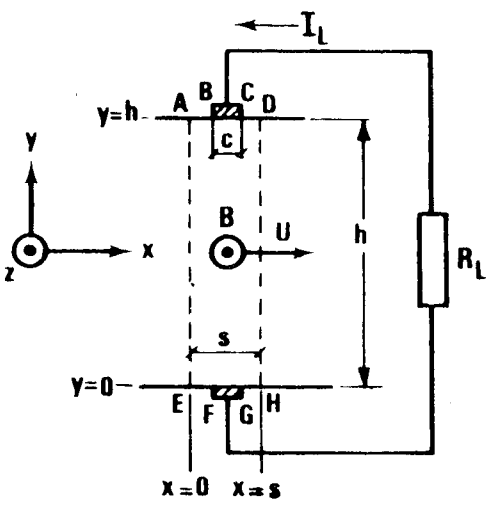

Fig. 1 Coordinate system and channel geometry used in the two-dimensional calculations.

4) All quantities are constant in the z direction.
5) The term $\nabla p_e/n_e$ in Ohm's law is negligible.
6) The thermal conduction term $\nabla \cdot q$, the radiation term Q_R, and all terms (including space derivatives) in the energy equation are negligible.
7) The electron temperature T_e is assumed to relax instantaneously.

The validity of these assumptions is checked in the previous work.[14]

Using the above assumptions, Eqs. (1-7) are reduced to the following set:

$$E_x = (1/\sigma)(j_x + \beta j_y) \tag{18}$$

$$E_y - uB = (1/\sigma)(-\beta j_x + j_y) \tag{19}$$

$$\frac{\partial j_x}{\partial x} + \frac{\partial j_y}{\partial y} = 0 \tag{20}$$

$$\frac{\partial E_y}{\partial x} - \frac{\partial E_x}{\partial y} = 0 \tag{21}$$

$$n_e = n_{ia} + n_{ic} \tag{22}$$

$$\frac{\partial n_{ia}}{\partial t} = \dot{n}_{ia} - u\frac{\partial n_{ia}}{\partial x} \tag{23}$$

$$\frac{\partial n_{ic}}{\partial t} = \dot{n}_{ic} - u\frac{\partial n_{ic}}{\partial x} \tag{24}$$

$$\frac{2}{3kn_eT_e}\cdot\frac{j_x^2+j_y^2}{\sigma} - \delta m_e\left(1-\frac{T}{T_e}\right)\times\left(\frac{\nu_a}{m_a}+\frac{\nu_{ia}}{m_{ia}}+\frac{\nu_c}{m_c}+\frac{\nu_{ic}}{m_{ic}}\right)$$
$$-\left(1+\frac{2\epsilon_{ic}}{3kT_e}\right)\frac{\dot{n}_{ic}}{n_e} - \left(1+\frac{2\epsilon_{ia}}{3kT_e}\right)\frac{\dot{n}_{ia}}{n_e} = 0 \tag{25}$$

Once gas quantities such as n_e and T_e are given in a certain moment, σ and β are obtained from Eqs. (8) and (9). Then the electrical quantities can be calculated from Eqs. (18-21) together with the boundary condition (to be discussed later). Having found the value of j_x and j_y, the gas quantities at the next time step can be found from Eqs. (22-25). By repeating this procedure for sequential time steps, the time-dependent behavior of the ionized plasma can be simulated.

Current Stream Function

The electrical quantities j_x, j_y, E_x, E_y can be solved directly from Eqs. (18-21). However, a current stream function is often introduced into the calculation for the purpose of reducing the number of unknowns. Here, we will introduce the current stream function ψ defined by

$$j_x = \frac{I_L}{w}\frac{\partial \psi}{\partial y} \qquad j_y = -\frac{I_L}{w}\frac{\partial \psi}{\partial x} \tag{26}$$

where I_L is the load current and w the channel width. Equation (20) is satisfied by Eq. (26) and an equation for ψ is developed substituting Eqs. (18), (19), and (26) into Eq. (21) as

$$\frac{\partial}{\partial x}\left(\frac{1}{\sigma}\frac{\partial \psi}{\partial x} + \frac{\beta}{\sigma}\frac{\partial \psi}{\partial y}\right) + \frac{\partial}{\partial y}\left(\frac{\beta}{\sigma}\frac{\partial \psi}{\partial x} + \frac{1}{\sigma}\frac{\partial \psi}{\partial y}\right) = 0 \tag{27}$$

This equation is solved in the (x,y) plane.

Since an elliptic equation is to be solved, the boundary conditions have to be specified over the perimeter of the calculation plane. For a channel with electrodes and insulators arranged in an infinitely long periodic structure as shown in Fig. 1, the periodicity can be assumed over one segment. Therefore, calculations are made in one segment region (AEHD) in Fig. 1. The boundary condition on the electrode is $E_x = 0$ and using Eq. (26), Eq. (18) becomes

$$\frac{\partial \psi}{\partial y} - \beta\frac{\partial \psi}{\partial x} = 0 \quad \text{(on BC and FG)} \tag{28}$$

On the insulators $j_y = 0$ is given and substitution of Eq. (26) yields

$$\psi = \text{const} \quad \text{(on AB, CD, EF, and GH)} \tag{29}$$

By definition ψ is taken equal to zero on the left insulator, namely

$$\psi = 0 \quad \text{(on AB and EF)} \tag{30}$$

The integration of j_y over the electrode gives the load current I_L; then

$$I_L = -w\int_B^C j_y \mathrm{d}x \tag{31}$$

Substituting Eq. (26) into Eq. (31) yields

$$I_L = w\int_B^C \frac{I_L}{w}\frac{\partial \psi}{\partial x}\mathrm{d}x = I_L[\psi(C) - \psi(B)]$$

Finally, we obtain

$$\psi(C) - \psi(B) = 1 \tag{32}$$

Then, by considering Eqs. (30) and (32), ψ must be unity on the right insulator, namely

$$\psi = 1 \quad \text{(on CD and GH)} \tag{33}$$

Since periodicity is assumed over the one segment, the boundary condition on DH and AE is given as,

$$\psi \text{ (on DH)} - \psi \text{ (on AE)} = 1 \tag{34}$$

The current stream function ψ is uniquely decided in one segment by solving the elliptic Eq. (27) with the boundary conditions given in Eqs. (28), (30), (33), and (34). A finite element method is used in the calculation. Each segment is divided into $40 \times 10 = 400$ rectangular elements ($\Delta x = 0.25$ m, $\Delta y = 4.0$ mm). In each element, the electron density, electron temperature, and current density are assumed to be constant.

Load Current

Having found the value of ψ, j_x and j_y are obtained from Eq. (26). However, in order to do this, the value of I_L should be known. By integrating Eq. (19) over the line $x = s/2$, we obtain

$$\int_0^h (E_y|_{x=s/2} - uB)\mathrm{d}y = \int_0^h \frac{1}{\sigma}(-\beta j_x + j_y)|_{x=s/2}\mathrm{d}y \tag{35}$$

Since each electrode is connected to a external load R_L as shown in Fig. 1, the next relation should be satisfied,

$$\int_0^h E_y|_{x=s/2}\mathrm{d}y = R_L I_L \tag{36}$$

Substituting this relation and Eq. (26) into Eq. (35) yields,

$$R_L I_L - uBh = -\frac{I_L}{w}\int_0^h \frac{1}{\sigma}\left(\beta\frac{\partial \psi}{\partial y} + \frac{\partial \psi}{\partial x}\right)\Big|_{x=s/2}\mathrm{d}y$$

Finally,

$$I_L = uBh \Big/ \left[R_L + \frac{l}{w} \int_0^h \frac{l}{\sigma} \left(\beta \frac{\partial \psi}{\partial y} + \frac{\partial \psi}{\partial x} \right) \Big|_{x=1/2s} \mathrm{d}y \right] \tag{37}$$

Here it is obvious that the second term of the denominator of the right-hand side of Eq. (37) corresponds to a internal resistance of the plasma. After calculating the value of I_L from this equation, we can obtain j_x and j_y from Eq. (26).

Plasma Quantities

Once the values of j_x and j_y are given in a certain period, the n_e, n_{ia}, n_{ic}, and T_e distributions at the next time step can be found from Eqs. (22-25). Equations (23) and (24) are integrated along their characteristics with a time step of 0.255 μs.

Gasdynamic and Geometrical Conditions

The gasdynamic conditions used in the calculations are taken to be equal to the experimental values obtained in the Eindhoven shock tunnel facility: stagnation temperature $T=2000$ K, Mach number $M=1.6$, static pressure at channel inlet $p=1.2$ atm, magnetic field $B=3$ T, load resistance $R_L=2\Omega$, and seed fraction $\epsilon=2\times10^{-4}$. From these conditions it follows that the gas static temperature $T=1079$ K, gas velocity $u=980$ m/s, argon number density $n_a=8.16\times10^{24}$ m^{-3}, and cesium number density $n_c=1.63\times20^{21}$ m^{-3}. Calculations under different load conditions ($R_L=0.02$-10Ω) are also performed. The dimensions of the channel have been chosen equal to two-fifths of the dimensions of an actual channel: channel height $h=40$ mm, channel width $w=40$ mm, one pitch length $s=10$ mm, and electrode width $c=4$ mm. (See Fig. 1.)

Linear Perturbation Analysis

The stability of the two-temperature plasma with respect to wave-like perturbations of the electron temperature and electron density was first studied by Kerrebrock.[5] Using linear perturbation analysis, he showed that under nonequilibrium conditions the argon cesium plasma is unstable if the Hall parameter exceeds a certain critical value. The following procedure is used in the calculation of the critical value of the Hall parameter. The gas pressure, gas temperature, and gas velocity u are taken to be constant. Fourier components of the disturbance for the unknowns n_e, T_e, j, and E are introduced,

$$n_e = n_{e0} + n_{e1} \exp[i(k \cdot r + \omega t)] \tag{38}$$

etc.

Using Eqs. (6) and (7) and the field equations (2) and (3), a dispersion relation can be derived that is quadratic in ω.[7] Second- and higher-order terms are neglected in the derivation. For simplification, the Saha equilibrium is assumed instead of the particle equation (6). Further, heat conduction and radiation loss are neglected. Solution of the equations yields the imaginary part ω_i of ω as a function of the zero-order values n_{e0}, T_{e0}, j_0, and E_0 and the direction of k.[6] It can be shown that for angles near 45 deg between k and j_0, ω_i has its maximum value for large values of β. In case this maximum value is taken equal to zero, the critical Hall parameter is[6,7]

$$\beta_{cr} = 2\sqrt{(K_0+1)(K_0+r_0)} \tag{39}$$

where

$$K_0 = \frac{1}{2} \frac{T_{e0}}{T_{e0}-T} \left(\frac{\mathrm{d}\ell n T_e}{\mathrm{d}\ell n n_e} \right)_0$$

$$r_0 = \left(\frac{\mathrm{d}\ell n \nu_e}{\mathrm{d}\ell n n_e} \right)_0 \tag{40}$$

The results shown in Eqs. (39) and (40) are found for cases where the electric field vector, current density vector, and wave vector k are perpendicular to the magnetic induction B.

Equation (39) shows that β_{cr} depends on the zero-order values of K_0 and r_0. These values can be calculated for a stationary and homogeneous nonequilibrium plasma. The dependence of β_{cr} and β on the electron temperature for the plasma that satisfies the gasdynamic conditions given in the previous section is calculated.

Figure 2 shows the calculated curves. It is found from this figure that the plasma is stable at electron temperatures between 4200 and 6500 K. This stable region corresponds to a regime of fully ionized seed. The electron temperature relates to the current density through Eq. (25) and the current density is coupled to the external load through Eq. (37). Therefore, the electron temperature can be controlled by changing the external load resistance. It can be understood from Eqs. (25) and (37) that the electron temperature increases with the decreasing external load resistance and decreases with the increasing resistance. This suggests that a stable plasma can be present in the channel by selecting the appropriate external load resistance.

However, these linear theories start with a homogeneous plasma; therefore, in order to obtain a stable plasma, the electron temperature distribution must not only be within the above range but also be homogeneous in the channel. However, in our case, the initial electron temperature is less than 2000 K since the actual stagnation gas temperature is limited to 2000 K; at this electron temperature, instability can develop in the channel. The question remains whether the homogeneous electron temperature distribution is present after the instability develops. In order to answer this question, time-dependent calculations should be made. The results of the calculations are presented in the next section.

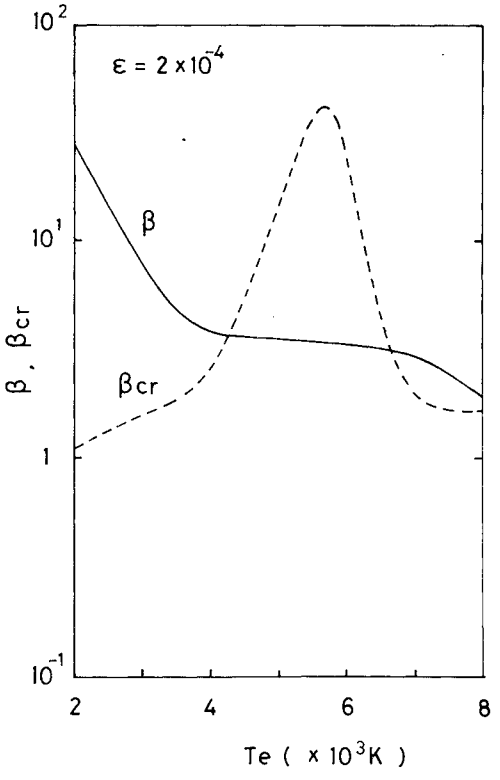

Fig. 2 Dependence on Hall parameter and critical Hall parameter on electron temperature.

Numerical Results

Streamer Development at Typical Case

In the first place, a numerical simulation of the streamer development in the channel is performed. The initial con-

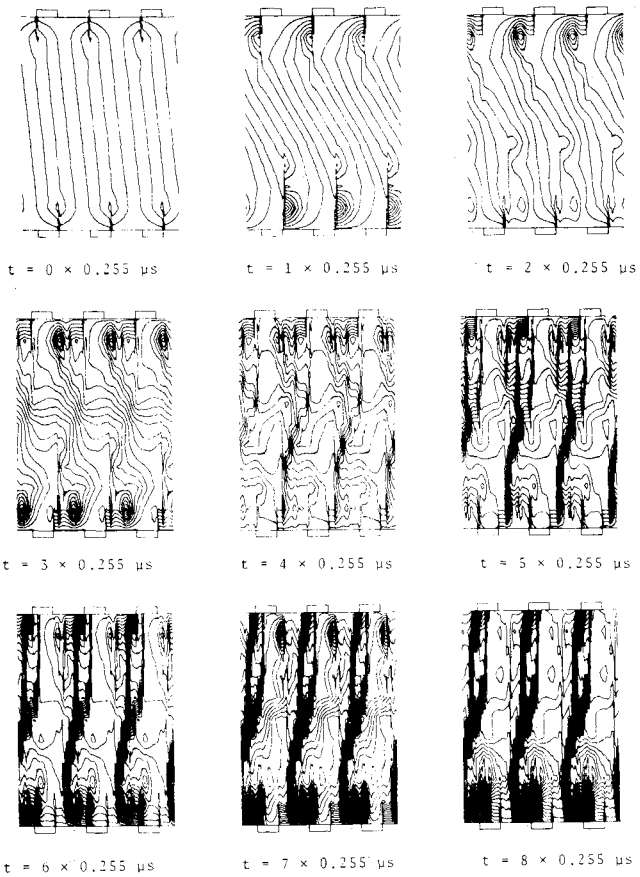

Fig. 3 Time-dependent current streamline distribution before the constricted discharge structure is formed (contour interval: $\Delta\psi = 0.1$ A).

ditions are defined as follows: for $t<0$ the plasma is assumed to be in Saha equilibrium with the electron temperature equal to the stagnation gas temperature. At $t=0$ the electrodes are connected to the external circuits. The time history of the current distributions at $t=0\text{-}8\times0.255$ μs is shown at different time steps in Fig. 3. Although the calculation is done in one segment, three segments are shown in the figures. The thin streamers are formed at approximately $t=8\times0.255$ μs.

The development of the streamer structures after they are initially formed is illustrated at six time instances ($t=10$, 20, 30, 50, 100, 200×0.255 μs) in Fig. 4. Note that the contour interval $\Delta\Psi$ taken in this figure is 10 times larger than Fig. 3. Electron density and electron temperature distributions at same time instances are also shown. The range of the electron density and the temperature in Fig. 4 is the same as the one shown in Fig. 5. The streamers are fully developed within 100×0.255 μs and are frozen in the gas and convected downstream at the gas velocity. Other noteworthy items are the following: inside the streamers, the electron density is in the range of $1.4\text{-}1.7\times10^{21}$ m^{-3} and the electron temperature is around 4000 K. Outside the streamers, the electron density is on the order of 10^{19} m^{-3} and the electron temperature is between 2000 and 3000 K. Since these results agree with the experimental results obtained from the shock tunnel facility, the inhomogeneous structure observed in the experimental facility can be explained as the result of nonlinear growth of ionization instabilities.

Load Change Characteristics of the Discharge Structure

The discharge structures for various load conditions are investigated and simulated. The final discharge structure, electron density, and electron temperature distributions in the channel are shown in Fig. 5 for four load conditions, namely $R_L=10$, 2, 0.2, and 0.02Ω.

In the case of $R_L=10\Omega$, the final discharge structure is a streamer mode similar to the case of $R_L=2\Omega$, but the number

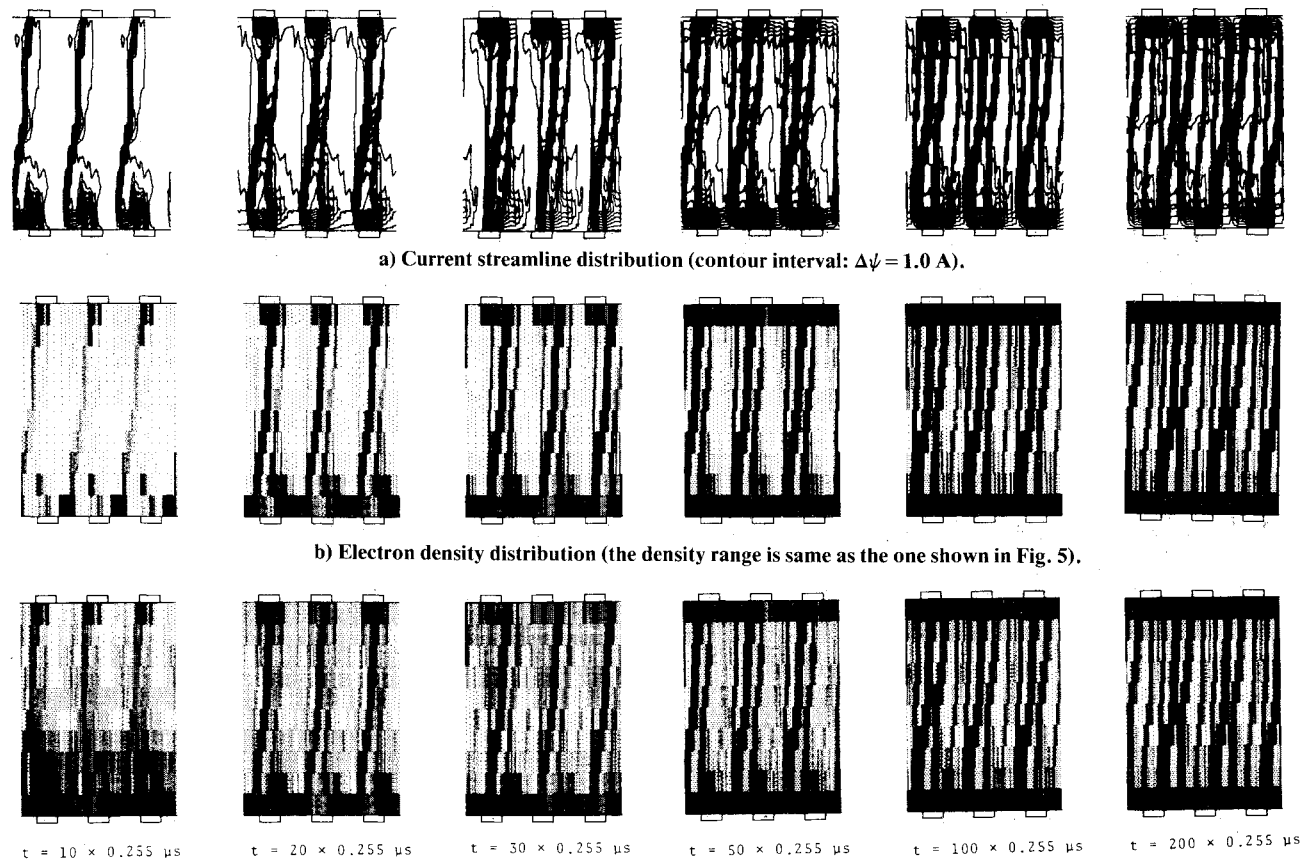

a) Current streamline distribution (contour interval: $\Delta\psi = 1.0$ A).

b) Electron density distribution (the density range is same as the one shown in Fig. 5).

c) Electron temperature distribution (the density range is same as the one shown in Fig. 5).

Fig. 4 Time-dependent current streamline, electron density, and electron temperature distribution after the initial formation of the constricted discharge

of streamers decreases. The electron density and the temperature in the streamers of this case are about 7.2×10^{20} m^{-3} and 3300 K, respectively, which are lower than those of the case where $R_L=2\Omega$. It can be said that the electron density and the electron temperature in the streamers increase with decreasing load resistance until the cesium is fully ionized.

Simulations are also performed for a load resistance of 0.2Ω. This corresponds to the condition of the fully ionized seed regime and from conventional linear theories a stable plasma is expected to be obtained in the channel. However, linear theories can predict only that the plasma remains homogeneous and stable if the homogeneous and stable plasma is produced under this condition. It cannot predict whether or not this kind of stable plasma can be produced starting with a plasma at a stagnation temperature around 2000 K. Therefore, the time-dependent numerical simulation is necessary in order to predict the possibility of realizing a homogeneous and stable plasma. The calculated time-dependent discharge structure of this case is shown in Fig. 6. The remarkable fact is that in this case, once streamers are formed in the channel, they gradually begin to spread out in time and cover the whole region of the channel until they become almost homogeneous. In this case, this means that ionization instabilities also occur initially, but in the end the plasma becomes homogeneous and stable. It is also seen from Fig. 5 that the electron density is about 1.7×10^{21} m^{-3} everywhere and the electron temperature is between 5500 and 6500 K. It should be noted that argon is rarely ionized in the streamer until the cesium is fully ionized in the whole region of the channel.

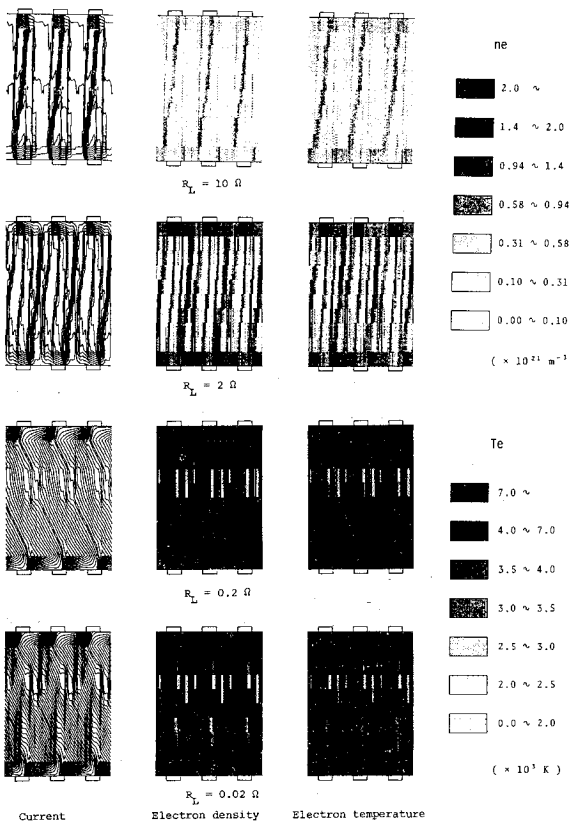

Fig. 5 Final distributions of current streamline, electron density, and electron temperature for various load resistances ($R_L=10, 2, 0.2, 0.02$ Ω).

The time-dependent discharge structure for relatively low load resistance, $R_L=0.02\Omega$, is illustrated in Fig. 7. Although the structure of this case is almost the same as in the case of $R_L=0.2\Omega$ at $t=0\text{-}100\times0.255$ μs, it changes after $t=100\times0.255$ μs and again becomes inhomogeneous. This is because argon will ionize in some parts of the channel, as seen in the electron density distributions of Fig. 5.

It is also found from Fig. 5 that the electron density distribution is closely connected with the electron temperature distribution and the Saha equilibrium relation is almost satisfied in the entire channel.

Effective Electrical Conductivity and Hall Parameter

The occurrence of ionization instabilities reduces the effective value of the electrical conductivity and the Hall parameter. The effective electrical conductivity $\sigma_{\text{eff}}=\langle j\rangle^2/\langle j\rangle\langle E^*\rangle$ and the effective Hall parameter $\beta_{\text{eff}}=\langle E^*\rangle_\perp/\langle E^*\rangle_{/\!/}$ are calculated from the simulated results of current density and the electric field distributions in the channel for different load conditions. The effective electrical conductivity is plotted for several load currents (i.e., load resistances) in Fig. 8. The average electrical conductivity $\langle\sigma\rangle$ and apparent electrical conductivity defined as

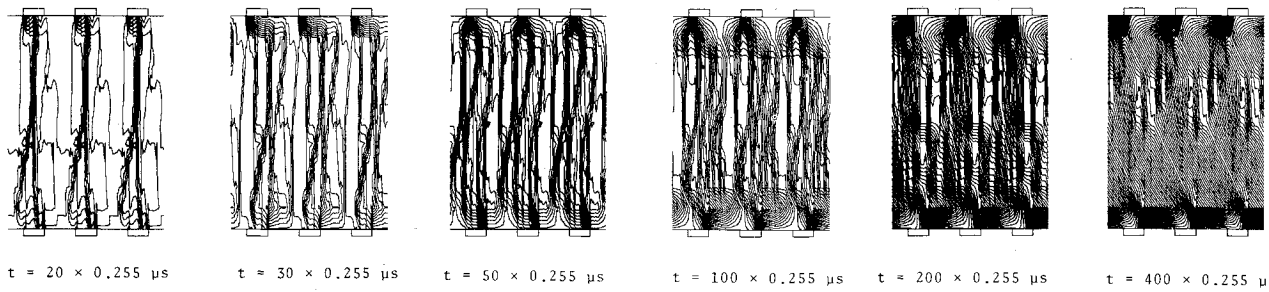

Fig. 6 Time-dependent current streamline distribution for $R_L=0.2\Omega$ (contour interval: $\Delta\psi=5.0$ A).

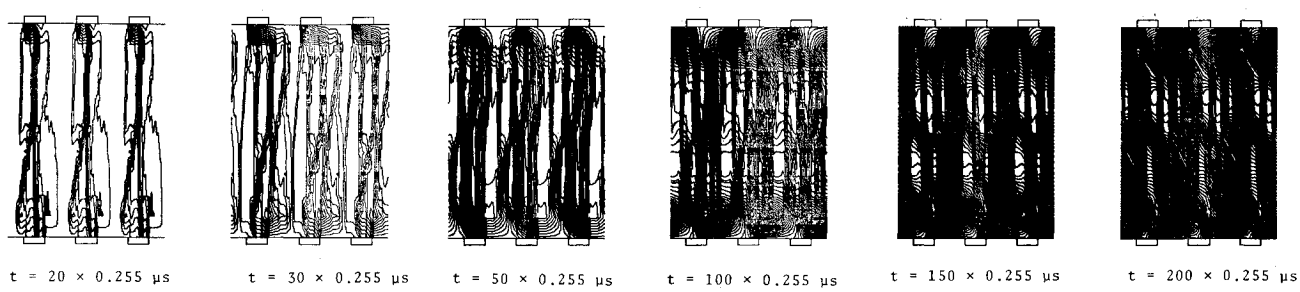

Fig. 7 Time-dependent current streamline distribution for $R_L=0.02\Omega$ (contour interval: $\Delta\psi=5.0$ A).

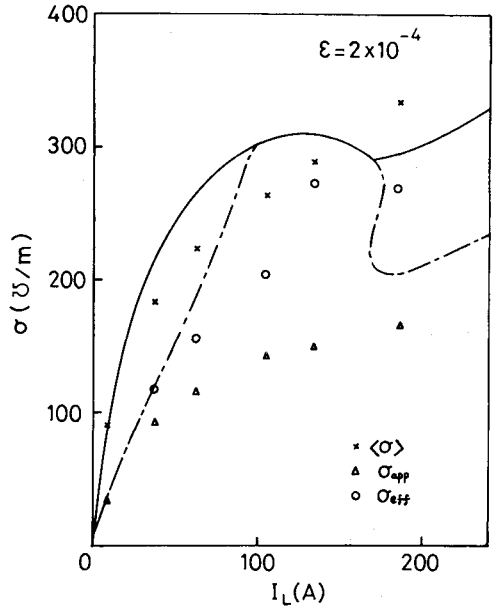

Fig. 8 Effective, apparent, and average electrical conductivities vs load current.

$\sigma_{app} = (I_y / V_y^*)(h/sw)$ are also plotted in the same figure. Furthermore, the ideal electrical conductivity is shown by the solid line and the effective electrical conductivity calculated from the conventional linear theory by the dashed line.

It is very interesting to note from Fig. 8 that the effective electrical conductivity obtained from the two-dimensional time-dependent simulation of the ionization instabilities shows the same tendency as the one obtained from the conventional linear theory, which assumes the steady-state condition. The effective electrical conductivity corresponding to a load resistance of 0.2Ω ($I_L = 120$ A) shows a close comparison to the ideal value. This indicates that under this load condition, the ionization instabilities do not exist in the channel and the plasma is stable.

The effective Hall parameter $\beta_{\text{eff}} = \langle E^* \rangle_\perp / \langle E^* \rangle_{/\!/}$ is also obtained from the simulation. The value of β_{eff} at $R_L = 0.2\Omega$ is about 2.0, but reduces to unity at $R_L = 2.0\Omega$, which means the effective Hall parameter becomes large under the stable condition.

Conclusions

This paper deals with a two-dimensional, time-dependent numerical simulation of the growth of streamers in MHD channels and results are obtained for different load conditions. The following conclusions are derived from our calculations:

1) The inhomogeneous discharge structure observed in the Eindhoven shock tunnel facility can be explained to be a result of the nonlinear growth of ionization instabilities.

2) For relatively large load resistance, the final discharge becomes a streamer structure.

3) For the certain small load resistances, almost homogeneous and stable discharge can be realized in spite of the fact that the initial state predicts the occurrence of ionization instability.

4) For relatively small load resistances, argon is ionized in some parts of the channel and the discharge becomes inhomogeneous.

5) The effective electrical conductivity for the case of a homogeneous plasma is greater than any other case and is close to the ideal value.

6) Under any load conditions, the electron density and the corresponding electron temperature satisfy the Saha equilibrium relation throughout the channel.

Acknowledgments

The authors wish to express their thanks to Prof. L. H. Th. Rietjens and Dr. A. Veefkind of Eindhoven University of Technology for their useful discussions and suggestions.

References

[1] Zauderer, B., "Discharge Structure and Stability of Nonequilibrium Plasma in a Magnetichydrodynamic Channel," *Physics of Fluids*, Vol. 11, Dec. 1968, pp. 2577-2585.

[2] Brederlow, G., Witte, K. J., and Zinko, H., "Investigations of the Discharge Structure in a Noble Gas Alkaki MHD Generator, Parts I and II," *AIAA Journal*, Vol. 11, Aug. 1973, pp. 1065-1079.

[3] Veefkind, A. et al., "Investigations of the Nonequilibrium Condition in a Shock-Tunnel Driven Noble Gas MHD Generator," *Proceedings of the 7th International Conference on MHD Electrical Power Generation*, Vol. 2, 1980, pp. 703-710.

[4] Veefkind, A., Sens, A. F. C., and Wetzer, J. M., "Shock Tube Investigation on MHD Conversion in Argon-Cesium," *Proceedings of the 19th Symposium on Engineering Aspects of MHD*, 1981, p. 7.3.1.

[5] Kerrebrock, J. L., "Nonequilibrium Ionization Due to Electron Heating, I: Theory," *AIAA Journal*, Vol. 2, June 1964, pp. 1072-1080.

[6] Solbes, A., "Quasi-Linear Plane Wave Study of Electrothermal Instabilities," *Proceedings of the 4th International Conference on MHD*, 1968, pp. 500-518.

[7] Nelson, A. H. and Haines, M. G., "Analysis of the Nature and Growth of Electrothermal Waves Q," *Plasma Physics*, Vol. 11, 1969, pp. 811-837.

[8] Velikhov, E. P. et al., "Numerical Experiment on Ionization Istability Development in a Low Temperature Magnetized Plasma," *Proceedings of the 10th Symposium on Engineering Aspects of MHD*, 1969, pp. 1-4.

[9] Lengyel, L. L., "Numerical Simulation of Ionization Instability with Allowance for Dissipative Processes," *Proceedings of the 11th Symposium on Engineering Aspects of MHD*, 1970, pp. 193-198.

[10] Uncles, R. J., "A Numerical Simulation of Electrothermal Waves," *Energy Conversion*, Vol. 14, 1975, pp. 103-110.

[11] Nakamura, T. and Riedmuller, W., "Stability of Nonequilibrium MHD Plasma in the Regime of Fully Ionized Seed," *AIAA Journal*, Vol. 12, May 1974, pp. 661-668.

[12] Yamasaki, H. and Shioda, S., "MHD Power Generation with Fully Ionized Seed," *Journal of Energy*, Vol. 1, Sept.-Oct. 1977, pp. 301-305.

[13] Shioda, S. et al., "Power Generation Experiments and Prospects of Closed Cycle MHD with Fully Ionized Seed," *Proceedings of the 7th International Conference on MHD Electrical Power Generation*, Vol. 2, 1980, pp. 685-695.

[14] Hara, T., Veefkind, A., and Rietjens, L. H. Th., "Numerical Simulation of the Inhomogeneous Discharge Structure in Noble Gas MHD Generators," *AIAA Journal*, Vol. 20, No. 11, 1982, pp. 1473-1480.

[15] Hara, T., Umoto, J., and Fujiwara, A., "Streamer Development in Noble Gas MHD Channels in Relation to Seed Fractions," *Proceedings of the 20th Symposium on Engineering Aspects of MHD*, 1982, p. 10.7.1.

[16] Spitzer, L., *Physics of Fully Ionized Gases*, Wiley Interscience, New York, 1956.